Direct numerical prediction of OH-LIF Signals in the Simulation of a laminar partial oxidation flame

F. Hunger*[1], B. Stelzner[2], D. Trimis[2], C. Hasse[1]

[1]Chair of Numerical Thermo-Fluid Dynamics, ZIK Virtuhcon, Technische Universität Bergakademie Freiberg, Freiberg, Germany

[2]Karlsruhe Institute of Technology, Engler-Bunte-Institute, Combustion Technology, Karlsruhe, Germany

Abstract

In the present study a laminar inverse partial oxidation oxy-fuel jet flame previously studied both experimentally and numerically [1,2,3,4] is investigated. Special emphasis is placed on the comparison of the OH-LIF signal. The OH-LIF signal was measured correcting for signal noise, PAH fluorescence and absorption. Equivalent OH-LIF signals are generated from the numerical data taking into account collisional quenching and the Boltzmann distribution. Both contributions are calculated based on the detailed local species and temperature distribution. The experimental and the numerical OH-LIF signal are directly compared in order to avoid potential inaccuracies when comparing the OH mole fraction being a post processed quantity in the experiment. Differences of the direct signal comparison in contrast to the comparison of the OH mole fraction are analyzed. The influence of collisional quenching and the Boltzmann distribution on the numerical signal is studied. Finally, the impact of different modeling approaches for radiation and diffusion is quantified regarding their sensitivity on the OH-LIF signal.

Introduction

The analysis of oxy-fuel systems and complex fuels such as dimethylether has become more important recently in numerical and experimental combustion investigations [5].

However, the experimental investigation of such systems is usually more complicated compared to methane-air combustion. Soot formation [6], significantly altered chemical paths [7,8,9] and high heat losses [10] due to substitution of N_2 by CO_2 introduces several challenges for experimentalists. Furthermore, the detailed analysis and quantification of all species participating in the conversion of higher hydrocarbons is more challenging [11].

Significant advances have been achieved to improve the interplay between experiments and numerics in order to better understand the underlying physical and thermo-chemical phenomena, see e.g. [12,13]. However, experimental measurements are usually post processed in order to obtain desired physical quantities, which can be compared to equivalent numerical results, which on the other hand depend on the underlying modeling assumptions e.g. for transport and radiation [14]. By this, potential inaccuracies, assumptions of data processing and model deficiencies are transferred to the experimental numerical comparison.

Looking specifically at OH-LIF measurements, the obtained signal depends on quenching with other participating species and the local temperature, both are generally unknown in OH-LIF experiments and its determination requires high effort. This makes the quantification of the OH mole fraction based on OH-LIF measurements prone to inaccuracies.

In order to avoid the issues of converting measurement data to physical quantities, the comparison of the actual experimental signal and the signal predicted by numerical simulations was suggested by [15]. The advantages of this procedure were identified to have simpler experiments requiring fewer measurements, and a better signal-to-noise ratio leading to reduced uncertainties. For turbulent flames, this approach is also important because simultaneous measurements of a sufficient number of quantities may not be possible. The authors applied the procedure to NO-LIF and luminosity measured from laminar sooting and non-sooting flames. A similar idea was also used for a turbulent flame in order to look at the CH_2O- and the OH-LIF signal [16].

Here, we follow this idea by directly comparing OH-LIF signal in an partial oxidation flame (POX-Flame) running a CH_4/CO_2 fuel mixture of 1:1 by mole volume with pure oxygen [1,2,3,4]. The OH-LIF signal based on the local mass fraction and temperature is compared to the experimental OH-LIF signal instead of the numerical OH mole fraction. The influence of the temperature distribution and the quenching correction is discussed.

Experimental Approach

Burner Setup

The partial oxidation flame is a laminar, inverse diffusion flame, developed by [3] as bench-scale problem of large-scale gasification processes. The oxidizer is fed as an inner jet and the fuel enters as surrounding co-flow.

The fuel is a CH_4/CO_2 mixture (1:1 by mole volume) and pure O_2 is used as oxidizer with a global equivalence ratio of $\Phi = 2.5$. The velocity profiles at the inlets were measured using laser Doppler anemometry (LDA) and these profiles were applied as boundary conditions in all CFD simulations, more details are given in [2].

1* Corresponding author: franziska.hunger@ vtc.tu-freiberg.de

Measurement Technique

For the OH-LIF measurements, the excitation with the $Q_1(8)$ line and the spectrally integrated detection of fluorescence in the (0-0) and (1-1) band of the electronic $A^2\Sigma\ X^2\Pi$ transition were used.

The presented OH profiles were averaged over 280 single shots. The fluctuation of the laser beam energy was recorded for each shot and equalized. Furthermore, excited PAH fluorescence was recorded for every axial position by detuning the laser wave length and subtracted from the LIF signal. Additionally, the integrated energy absorption along the radial position of the measurement plane was taken into account. Rotational symmetry of the flame was assumed for the local absorption correction.

Numerical Evaluation of the LIF Signal

The governing transport equations for the density ρ, the velocity ***u***, the total enthalpy *h* and the species mass fractions Y_i were solved directly for this laminar flame. Different models for diffusion and radiation are investigated and compared. More details on the numerical approach can be found in [2,4,17]. Note that the previous investigations showed the necessity to consider detailed full multi-component diffusion modeling via a mixture-averaged approach and to consider the Soret effect [1,2]. Further, radiation modeling applying spherical harmonics (P1) or the modified differential approximation (MDA) with a weighted sum of gray gases (WSGG) or a spectral line-based weighted sum of gray gases (SLW) approach for the radiative properties was found to be the best choice for this oxy-fuel setup [4]. Based on these findings the following investigations of the OH-LIF signal were performed.

In order to analyze potential measurement errors and the sensitivity of the different numerical approaches, the LIF signal was numerically evaluated.

The LIF signal S_{LIF} is a function of temperature *T*, pressure *p* and the number density in the ground state N_{OH}^0. It can be expressed with

$$S_{LIF}=C_{exp}I_{Laser}N_{OH}^0(p,T)f_{v,J}(T)B_{12}\Gamma(p,T)\Phi, \quad (1)$$

where C_{exp} is the experimental calibration factor, $f_{v,J}$ is the Boltzmann fraction of the rotational energy state *J* and the vibrational energy state *v*, B_{12} is the Einstein coefficient for absorption, Γ(p,T) is the overlapping integral for the excited lines and Φ is the quantum yield.

Assuming C_{exp}, I_{Laser} and B_{12} to be constant and considering the rotational Boltzmann fraction f_J only, Eq.(1) can be simplified. Further, no overlapping of lines was detected for the $Q_1(8)$ line. Thus, Γ(p,T) can be set equal 1. Since we are only interested in normalized quantities as will be shown later, Eq.(1) becomes

$$S_{LIF} \sim N_{OH}^0(p,T)f_J(T)\Phi. \quad (2)$$

The calculation of the quantum yield requires the Einstein coefficient for emission A_{21}, predissociation, photoionization and quenching Q_{21}. However, neglecting predissociation and photoionization as these are much smaller than quenching and assuming $A_{21}<<Q_{21}$, the quantum yield is dominated by collisional quenching Q_{21}. The quenching can be calculated with the quenching rate coefficient and the total number density of the deactivating species i. Correlations for the quenching rate coefficient are available in the literature. In the following calculation, the correlation and quenching cross section for OH according to [18] were used. The quenching species CH_4, CO, CO_2, H_2, H_2O, O_2, N_2 and OH were considered.

Finally, the Boltzmann distribution is evaluated according to [14].

The specific data chosen according to the excited molecule and the excitation state are listed in Tab.1.

Table 1: Specific input data for the OH-LIF of the $Q_1(8)$-line of the (1-0) vibrational band of the electronic $A^2\Sigma\ X^2\Pi$ transition.

Variable	Value
A_{21} for (0-0)	639800 s^{-1}
x_i	[18]
$\sigma_{Q,\infty,i}$	[18]
ε/k	[18]
B_v	1891 m^{-1}

Results

Following the procedure outlined above, the OH-LIF signal is compared for a methane-air, a methane-O_2 and the POX-Flame mixture in a non-premixed counter flow diffusion flame with constant inlet velocities of 0.1 ms^{-1} and low strain rates applying the GRI3.0 reaction mechanism [20] in order to investigate potential differences between air and oxy-fuel combustion. Due to the absence of nitrogen in oxy-fuel flames significant higher concentrations of quenching species like water may alter the quenching behavior. In contrast to methane-air combustion, higher flame temperatures lead to different Boltzmann distributions and a different temperature insensitivity of the collisional quenching [19]. Its influence is shown in Fig.1.

In general, differences in the appearance of the OH-LIF signal in contrast to the OH mole fraction can be seen. However, these differences are much more pronounced in oxy-fuel combustion. When methane-air combustion is examined, the differences in the normalized profiles are almost negligible on the fuel side and also small on the oxidizer side. In contrast, a pure methane-O_2 mixture as well as the mixture used for the POX-Flame, exhibit larger differences, which are again much more pronounced on the oxidizer side than on the fuel side. Thus, a direct comparison of the experimental and numerical signal can be advantageous,

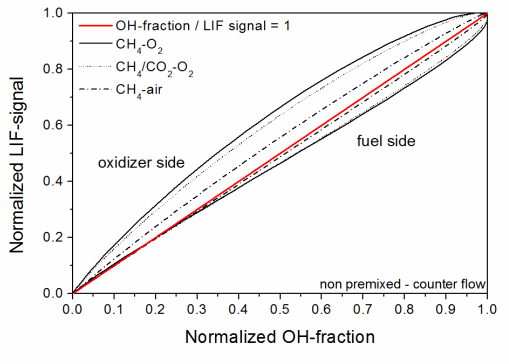

Figure 1: Comparison of the OH-LIF Signal and the OH mole fraction in a counter flow diffusion flame for methane-air combustion and two mixtures of oxy-fuel combustion.

especially in such oxy-fuel flames.

An analysis of the quenching species showed, that in case of air combustion approximately 50% of the collisional quenching is caused by N_2 and 40% by H_2O at the location of the maximum temperature. In case of oxy-fuel, H_2O reveals with 63% the strongest quencher. Additionally, OH quenches itself with 13%. In the CH_4/CO_2-O_2-flame the quenching species are H_2O and CO_2 and OH with 55%, 20% and 7%, respectively.

Further, the results for the POX-Flame are analyzed in the following section. Here, the numerical solution is based on the detailed simulation giving the best agreement found in the previous investigations using a mixture-averaged formulation including the Soret effect for diffusion modeling and the MDA approach together with SLW for the evaluation of the radiative heat transfer respectively.

The Boltzmann distribution and quenching results as well as the complete LIF-signal in comparison with the actual OH mole fraction are shown for the whole CFD domain in Fig.2.

For the Boltzmann fraction of the rotational level J = 8, illustrated in Fig.2 on the left, a broad range of the maximum value of 0.085 is obtained in the flame zone.

The Boltzmann fraction further exhibits sharp gradients in the mixing area of fresh fuel and oxidizer with hot reaction products caused by large gradients in the temperature distribution. However, over a wide range, the distribution of the Boltzmann fraction is almost constant since the excitation state chosen here is temperature-independent in the temperature range of 1000 to 3000 K [1].

Further, the collisional quenching is shown in the middle plot in Fig.2 indicating the area where quenching is important. Note that the collisional quenching is here restricted to the area where OH exists. Collisional quenching varies over a wide area and thus influences the OH-LIF signal significantly.

The comparison between the normalized OH mole fraction and the OH-LIF signal is shown in the right plot of Fig.2. Differences between the OH mole fraction and the OH-LIF signal are evident and expected. Thus, a conversion of the experimental LIF signal to the actual OH mole fraction, even after normalizing, is not straight-forward and requires a careful data analysis of the experimental signal.

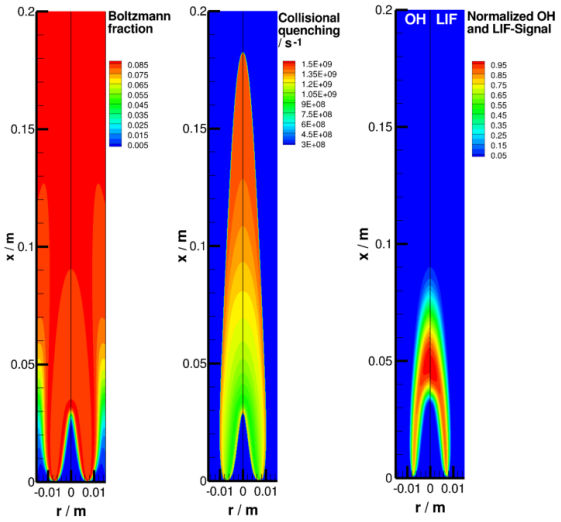

Figure 2: Contour plots of the Boltzmann fraction, the collisional quenching and the normalized LIF signal in comparison with the OH mole fraction in the burner domain up to a height of 0.2 m.

In order to quantify these results, Fig.3 shows the comparison between the numerical and experimental results. The LIF signal with and without taking collisional quenching into account are compared with the numerical OH mole fraction.

Even after normalizing, the OH-LIF signal is not similar to the mole fraction due to the above discussed collisional quenching.

In general, good agreement is found between the experimental OH-LIF signal and the numerical data. Note, that the normalization of the values is performed in every height and along the axis independently for both experiments and simulation. Further, as the mixture is homogenizing and the OH concentration is decreasing very much, all profiles agree well further downstream. Thus for the following analysis, we show the profiles along the axis and in three different slices within the flame zone. Here, we already found the profiles at a height of 80 mm to agree perfectly.

However, we clearly see the differences between the different signals and the OH distribution in the other plots. Starting with the signal neglecting collisional quenching, only the temperature dependence is captured via the Boltzmann fraction. The corresponding profiles are shifted towards the oxidizer jet (burner central axis). Taking the collisional quenching into account further intensifies this effect. The OH mole fraction and the actual OH-LIF signal thus show significant differences. It is important to note that the profiles in 40 mm height indicate the transition from the flame arms to the closed flame tip and are thus very sensitive to small alterations.

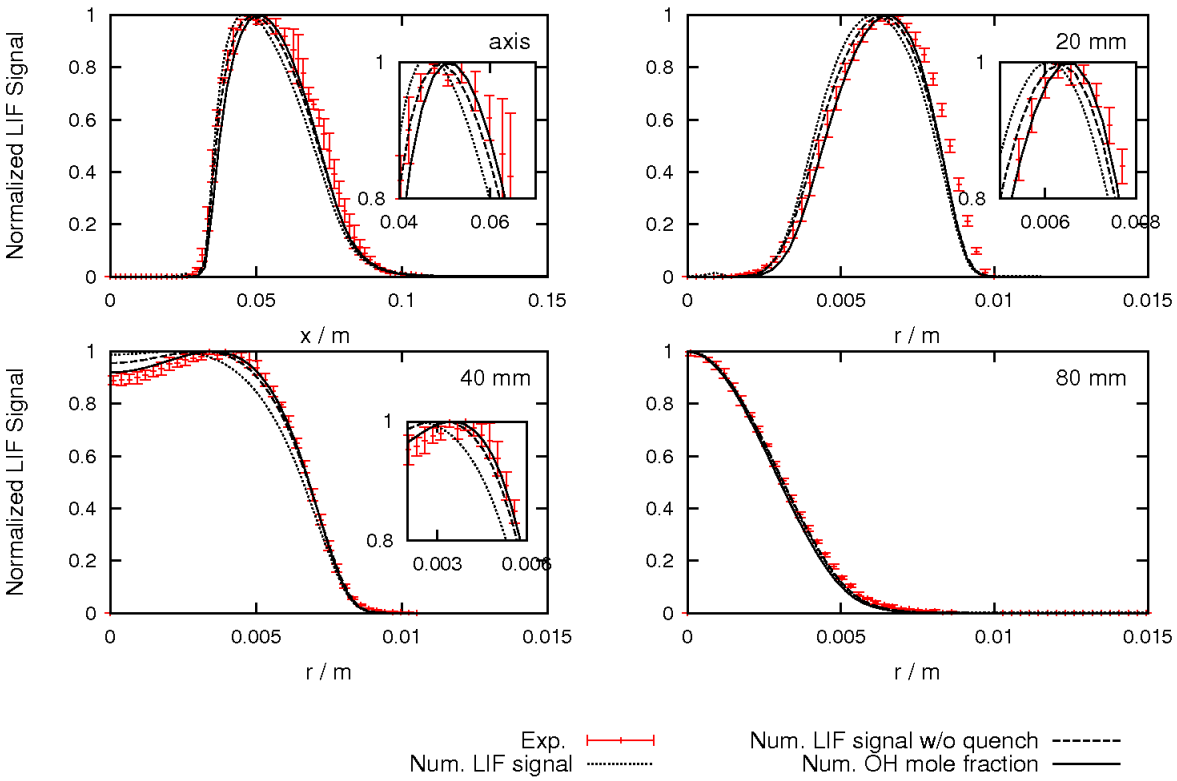

Figure 3: Comparison of the normalized experimental (not quenching corrected) and the two numerical LIF signals (w and w/o quenching correction) as well as the numerical OH mole fraction.

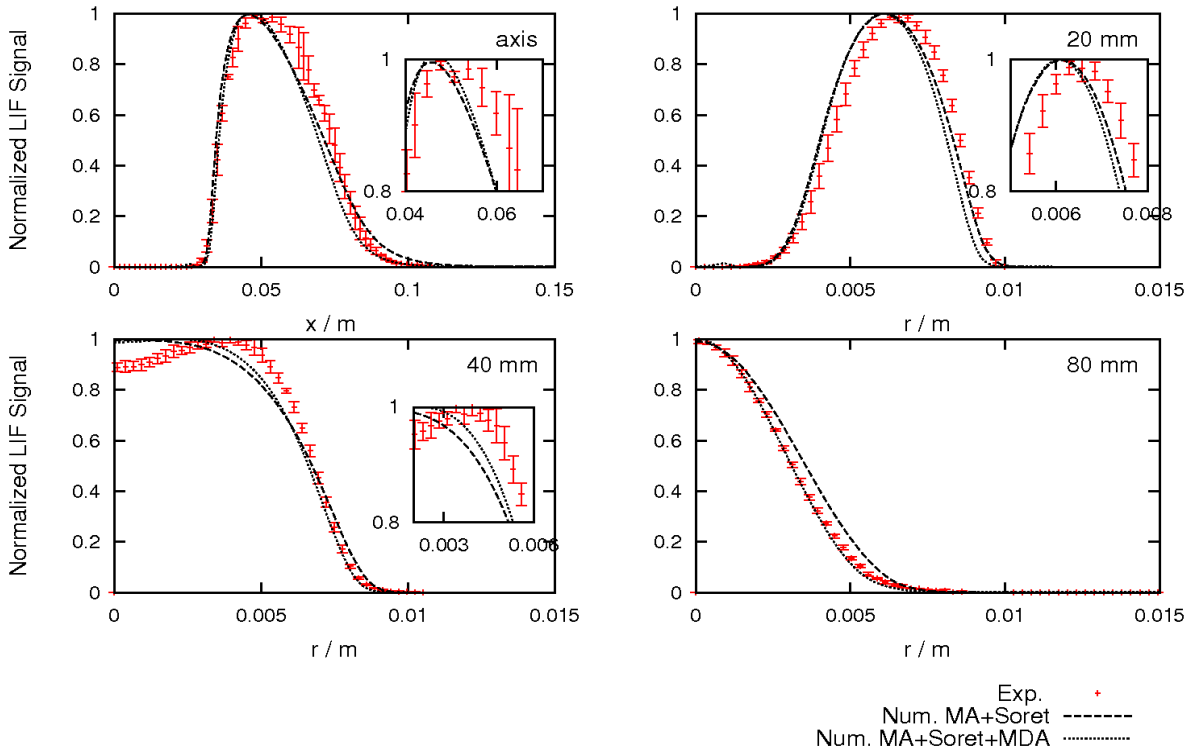

Figure 4: Comparison of the normalized experimental (not quenching corrected) and the numerical LIF signals (quenching correction) of simulations without radiation and with the MDA radiation model.

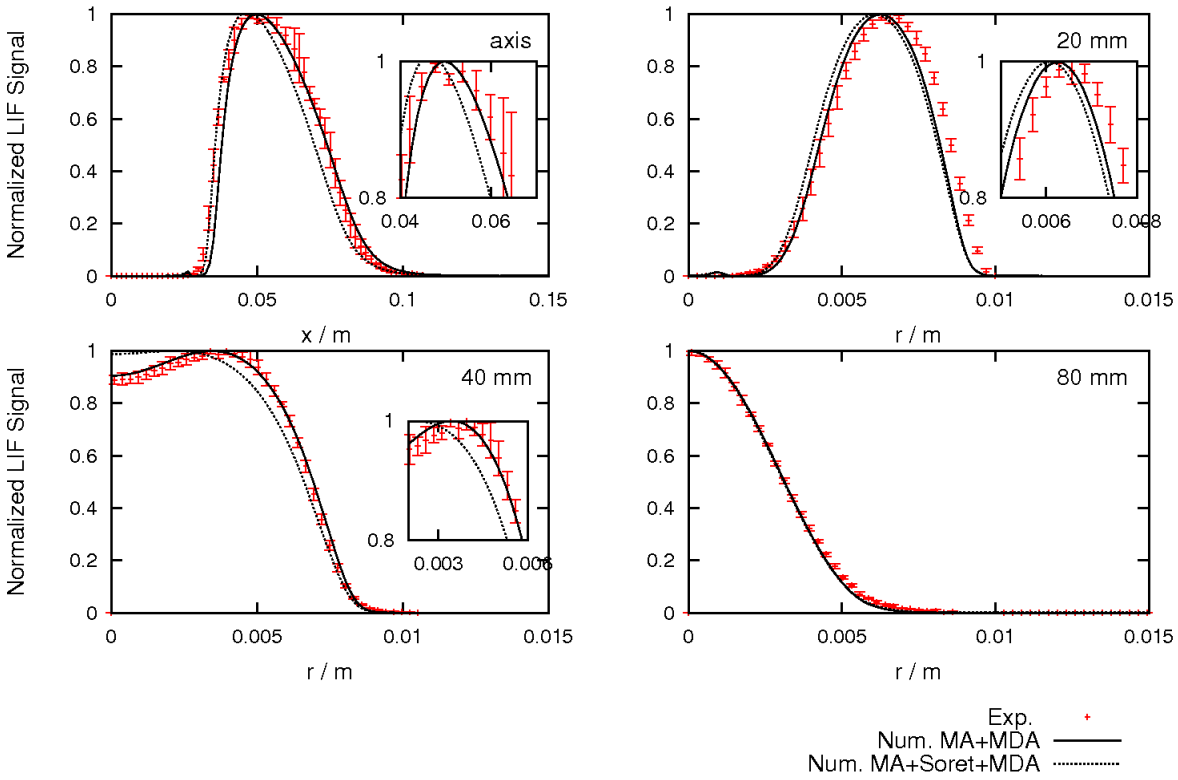

Figure 5: Comparison of the normalized experimental (not quenching corrected) and the numerical LIF signals (quenching correction) of simulations with and without the Soret effect.

In the following section, we aim to quantify the influence of the modeling approaches on the numerical LIF signal, here specifically the radiation and the thermal diffusion, respectively. First, the influence of the radiation model on the OH-LIF signal is shown in Fig.4.

Radiation modeling shifts the temperature level and thus also indirectly influences the OH mole fraction.

From Fig.4 it can be seen where differences can be found. The differences are small in the region of maximum signal but decrease further downstream and also towards the burner wall, which is particularly evident at a height of 80 mm. Here, much better agreement is obtained when radiation is considered. This is consistent with the findings of [4], where only the temperature profiles were compared.

Further, the influence of the Soret effect, which directly effects the species distribution, is investigated in Fig.5. A significant shift of the signal distribution along the burner middle axis can be seen. A much narrower signal profile is obtained when thermal diffusion is considered. However, these effects decrease further downstream.

When the Soret effect is included, the numerical signal is shifted towards the experimental signal. This is most evident along the burner central axis. Including radiation modeling still shifts the signal profiles and results in the best agreement between the numerical and the experimental OH-LIF signal.

Note that the differences occurring due to different modeling approaches are here in the same order of magnitude as differences due to differences in the evaluation of the numerical signal, c.f. Fig.3. This shows the influence of temperature distribution within the distribution of the Boltzmann fraction and collisional quenching and indicates the sensitivity of such experimental/numerical comparisons.

Conclusion

In the present study a laminar inverse partial oxidation oxy-fuel jet flame was investigated experimentally and numerically with special emphasis on the comparison of the OH-LIF signal. The OH-LIF signal was measured especially correcting for absorption.

On the other hand numerical OH-LIF signals were computed from the species data and temperature taking into account collisional quenching and the Boltzmann distribution.

A counter flow diffusion flame considering methane-air combustion and oxy-fuel combustion showed a higher influence of the collisional quenching on the OH-LIF signal for the oxy-fuel flame.

The comparison between the two different OH-LIF signals in the POX-Flame showed generally very good agreement confirming that such a direct comparison is feasible. The influence of the collisional quenching, the temperature and the Boltzmann distribution on the

flame structure was quantified. Especially the collisional quenching significantly shifted the signal in comparison to the numerical OH mole fraction. Thus the importance of collisional quenching correction in oxy-fuel processes was shown.

After establishing the general feasibility of such an approach for this specific flame, two modeling approaches were analyzed in detail for which it was previously shown that they have significant influence on the flame. The influence of radiation and diffusion modeling showed the sensitivity of the OH-LIF signal to these models. The differences of the modeling procedure were found to have the same order of magnitude as the influence of quenching correction and in the generation of the numerical signal.

In general, it could be confirmed that the comparison of experimental OH-LIF signals with numerically predicted signals is a feasible approach. Confidence in model validation using this approach is improved as the traditional assumptions required to capture collisional quenching and Boltzmann distribution are removed and are evaluated exactly within the numerical approach. Further, a higher sensitivity of the signal to modeling approaches is obtained due to the influence of temperature and species within the signal leading to a more detailed numerical/experimental comparison.

Acknowledgement

The authors would like to gratefully acknowledge the financial support by the German Research Foundation (DFG) for measuring equipment under HBFG programme INST 267/43-1 FUGG and HBFG programme INST 267/44-1 FUGG, by the Federal Ministry of Economics and Technology of Germany in framework of COORVED (project number: 0327865) and by the Federal Ministry of Education and Research of Germany in framework of Virtuhcon (project number 03Z2FN11).

References

[1] Stelzner, B., Hunger, F., Voss, S., Keller, J., Hasse, C., Trimis, D., Proceedings of the Combustion Institute 34 (2013) 1045–1055.
[2] F. Hunger, B. Stelzner, D. Trimis, C. Hasse, Flow, Turbulence and Combustion 90 (2013) 833–857.
[3] B. Stelzner, F. Hunger, A. Laugwitz, M. Gräbner, S. Voss, K. Uebel, M. Schurz, R. Schimpke, S. Weise, S. Krzack, D. Trimis, C. Hasse, B. Meyer, Fuel Processing Technology 110 (2013) 33–45.
[4] B. Garten, F. Hunger, D. Messig, B. Stelzner, D. Trimis, C. Hasse, International Journal of Thermal Sciences 87 (2015) 68–84.
[5] International workshop on measurement and computation of turbulent flames, http://www.sandia.gov/TNF/abstract.html, 2012.
[6] H. Wang, B. Dlugogorski, E. Kennedy, Combustion and Flame (2002).
[7] J. Park, J. S. Park, H. P. Kim, J. S. Kim, S. C. Kim, J. G. Choi, H. C. Cho, K. W. Cho, H. S. Park, Energy Fuels 21 (2007) 121–129.
[8] S. Linow, A. Dreizler, J. Janicka, E. P. Hassel, Measurement Science and Technology 13 (2002) 1952.
[9] P. Glarborg, L. L. B. Bentzen, Energy & Fuels 22 (2007) 291–296.
[10] J. M. Samaniego, T. Mantel, Combustion and flame 118 (1999) 537–556.
[11] F. Fuest, R. S. Barlow, J.-Y. Chen, A. Dreizler, Combustion and Flame 159 (2012) 2533–2562.
[12] R. S. Barlow, Proceedings of the Combustion Institute 31 (2007) 49 – 75.
[13] B. Böhm, J. Brübach, C. Ertem, A. Dreizler, Flow, Turbulence and Combustion 80 (2008) 507–529.
[14] A. C. Eckbreth, Laser Diagnostics for Combustion Temprature and Species, volume 3, Combustion Science and Technology Book Series, 1996.
[15] B. Connelly, B. Bennett, M. Smooke, M. Long, Proceedings of the Combustion Institute 32 (2009) 879 – 886.
[16] B. Coriton, M. Zendehdel, S. Ukai, A. Kronenburg, O. T. Stein, S.-K. Im, M. Gamba, J. H. Frank, Proceedings of the Combustion Institute (2014).
[17] D. Messig, F. Hunger, J. Keller, C. Hasse, Combustion and Flame 160 (2013) 251–264.
[18] M. Tamura, P. A. Berg, J. E. Harrington, J. Luque, J. B. Jeffries, G. P. Smith, D. R. Crosley, Combustion and Flame 114 (1998) 502 – 514.
[19] P.H. Paul, J. Quant. Spectrosc. Radiat. Transfer 51 (1994) 511-524.
[20] G.P. Smith, D.M. Golden, M. Frenklach, N.W. Moriarty, B. Eiteneer, M. Goldenberg, C.T. Bowman, R.K. Hanson, S. Song, W.C. Gardiner, V.V. Lissianski, Z. Qin, available at: http://www.me.nerkley.edu/gri_mech/